Agricultural Water Management 204 (2018) 247–261

Contents lists available at ScienceDirect

Agricultural Water Management

journal homepage: www.elsevier.com/locate/agwat

Evaluation of olive response and adaptation strategies to climate change under semi-arid conditions

I.J. Lorite[a,*], C. Gabaldón-Leal[a], M. Ruiz-Ramos[b], A. Belaj[a], R. de la Rosa[a], L. León[a], C. Santos[a]

[a] Andalusian Institute of Agricultural Research and Training (IFAPA), Centre "Alameda del Obispo", Córdoba, Spain
[b] Research Centre for the Management of Agricultural and Environmental Risks, Technical University of Madrid, Spain

ARTICLE INFO

Keywords:
Irrigation requirements
Yield
Irrigation water productivity
Olive
Climate change

ABSTRACT

AdaptaOlive is a simplified physically-based model that has been developed to assess the behavior of olive under future climate conditions in Andalusia, southern Spain. The integration of different approaches based on experimental data from previous studies, combined with weather data from 11 climate models, is aimed at overcoming the high degree of uncertainty in the simulation of the response of agricultural systems under predicted climate conditions.

The AdaptaOlive model was applied in a representative olive orchard in the Baeza area, one of the main producer zone in Spain, with the cultivar 'Picual'. Simulations for the end of the 21st century showed olive oil yield increases of 7.1 and 28.9% under rainfed and full irrigated conditions, respectively, while irrigation requirements decreased between 0.5 and 6.2% for full irrigation and regulated deficit irrigation, respectively. These effects were caused by the positive impact of the increase in atmospheric CO_2 that counterbalanced the negative impacts of the reduction in rainfall. The high degree of uncertainty associated with climate projections translated into a high range of yield and irrigation requirement projections, confirming the need for an ensemble of climate models in climate change impact assessment.

The AdaptaOlive model also was applied for evaluating adaptation strategies related to cultivars, irrigation strategies and locations. The best performance was registered for cultivars with early flowering dates and regulated deficit irrigation. Thus, in the Baeza area full irrigation requirements were reduced by 12% and the yield in rainfed conditions increased by 7% compared with late flowering cultivars. Similarly, regulated deficit irrigation requirements and yield were reduced by 46% and 18%, respectively, compared with full irrigation. The results confirm the promise offered by these strategies as adaptation measures for managing an olive crop under semi-arid conditions in a changing climate.

1. Introduction

Olive constitutes the main economic and social crop in numerous areas of the region of Andalusia (southern Spain). Currently, Andalusia is the main olive oil producer in the world and olive cultivation is almost the sole economic driver in many areas of this region. Recently, there has been growing concern about the future sustainability of this agricultural system (Gómez-Limón and Riesgo, 2010; Fernández-Escobar et al., 2013). In this regard, the installation of irrigation systems in traditional rainfed olive orchards in Andalusia during the 1990s resulted in a significant increase in yields and inter-annual yield stability (Sanchez-Martinez and Paniza, 2015). However, despite the huge effort made by farmers and public institutions, vast olive growing areas of Andalusia still have deficient irrigation water management. This, together with other factors such as high energy costs, result in a low profitability (Lanzas and Moral, 2008; Parras, 2013), which is threatening the sustainability of this agricultural system.

In this context, the impact of climate change on olive orchards located in semi-arid regions such as Andalusia could generate severe economic losses, and even lead to the disappearance of this crop in many areas (Areal and Riesgo, 2014). To identify adaptation strategies for olive orchards, the first step is the development of a robust simulation approach for evaluating olive crop behavior under baseline and future climate conditions. To date, however, olive modeling has been limited. Three clear methodologies have been used to assess crop development, yield and irrigation requirements: the first is based on complex physiological approaches (Villalobos et al., 2006; Morales et al., 2016), the second applies a simplified focus based on crop coefficients (Allen et al., 1998; Clarke et al., 1998), and the third employs statistical models such as the one described by Quiroga and

* Corresponding author.
E-mail address: ignacioj.lorite@juntadeandalucia.es (I.J. Lorite).

https://doi.org/10.1016/j.agwat.2018.04.008
Received 1 May 2017; Received in revised form 17 March 2018; Accepted 7 April 2018
Available online 30 April 2018
0378-3774/

Iglesias (2009). However, despite the advanced methodologies that have been developed for the characterization and evaluation of Mediterranean olive orchards (Santos et al., 2012), numerous uncertainties undermine the quality of the simulation results.

Regardless of the methodology applied, phenology is a crucial component of any study related to olive and climate change. Thus, Ayerza and Sibbett (2001) and Rapoport et al. (2012) considered flowering as a key phenological stage for final oil yield. Therefore, the likely occurrence of high temperatures and/or water stress (due to normal or extreme events) during this period would have a strong impact on irrigation scheduling and olive oil production. However, the existing uncertainties about the impact of climate change on olive phenology (Osborne et al., 2000; De Melo-Abreu et al., 2004; Oteros et al., 2013) require the development of new phenological models able to simulate the crop's response under future climate conditions (Gabaldón-Leal et al., 2017).

Besides phenology, a key process for olive yield is water management. The assessment of future irrigation requirements of olive orchards has generally involved simplified and statistical approaches (Rodríguez-Díaz et al., 2007; Tanasijevic et al., 2014). However, due to the limited available knowledge of the physiological response of the olive crop under future climate conditions, these approaches fail to account for several important processes such as the impact of an increase in atmospheric CO_2 or the interactions between phenology and heat and water stress.

The above mentioned limitations make climate change impact assessments prone to a high degree of uncertainty, primarily arising from the field data, the crop modeling and the climate projections. The quality and quantity of available field data means that there is limited existing knowledge about olive and, therefore, few crop models able to accurately reproduce olive development and growth. The crop and climate model-related uncertainty can be partially handled by ensemble modeling, which has proven to be an efficient alternative (Ruiz-Ramos et al., 2011; Pirttioja et al., 2015; Ruiz-Ramos et al., 2018). In this study, the lack of simulation models for olive able to simulate future climate conditions has been tackled by integrating simplified physically-based approaches based on experimental data to obtain a new simulation model named AdaptaOlive. Thus, data on key components such as phenology, atmospheric CO_2 effects on transpiration efficiency or the impact of water stress during flowering on yield have been considered. In addition, the AdaptaOlive model with an ensemble of bias-corrected regional climate projections (Dosio et al., 2012) has been applied for the first time in order to assess future olive crop response to climate change, and the related uncertainty.

The objectives of this study were: 1) to assess the impact of climate change on yield, water requirements and economic components of traditional Mediterranean olive orchards by means of a simulation model based on experimental data from previous studies, and 2) to identify the most suitable strategies for climate change adaptation for the olive crop under semi-arid conditions by analyzing a number of climate projections, olive genotypes, irrigation management strategies and locations within Andalusia.

2. Material and methods

2.1. Study area and climate

Andalusia displays a high variability of climate conditions, ranging from rainy areas with moderate temperatures (lower section of the Guadalquivir Valley) to warm and arid areas (east of the region). To represent this spatial climate variability, eight Andalusian locations were selected (Fig. 1): Antequera, Baena, Baeza, Córdoba, Martos, Osuna and Seville, all located within the traditional Andalusian olive-growing area; and Jerez, which lies outside it but is a future alternative olive-cultivating area, albeit probably affected by potential limitations related to fulfilling chilling requirements (Gabaldón-Leal et al., 2017).

Baseline and future climate simulations of the Andalusian climate were taken from 11 Regional Climate Models (RCMs) from the European project ENSEMBLES (http://ensembles-eu.metoffice.com) for the SRES A1B scenario (Nakićenović et al., 2000). The climate models (RCM driving GCM) used were DMI_ARPEGE, DMI_BCM, ETHZ, C4I_HadCM3Q16, HC_HadCM3Q0, KNMI, MPI, Reshaped CNRM_ARPEGE, SMHI_BCM, SMHI_ECHAM5 and SMHI_HadCM3Q3. For each one, outputs of daily weather data (minimum and maximum temperature, precipitation, relative humidity, solar radiation and wind speed), grouped in three temporal periods – baseline (B), from 1981 to 2010, near future (NF) from 2021 to 2050 and far future (FF) from 2071 to 2100 – were taken for the 145 cells composing Andalusia, with a cell size of 625 km^2 (25 × 25 km) each. RCM output was corrected for temperature and precipitation by a bias-correction technique (Dosio and Paruolo, 2011) consisting of the construction of a transfer function with modeled and observed daily mean, minimum and maximum temperature, and total precipitation. The observed gridded data used as a reference for the bias correction was the database SPAIN02 (Herrera et al., 2012), a gridded dataset developed for continental Spain and the Balearic Islands with 2756 quality-controlled stations, covering the period from 1950 to 2007, with a spatial resolution of 25 km. The corrected ensemble of RCM projections is hereafter referred to as ENS-SP (Ruiz-Ramos et al., 2015). The daily reference evapotranspiration was calculated following the Penman-Monteith approach (Allen et al., 1998). This study used mean annual atmospheric CO_2 concentrations based on measurements made at Mauna Loa Observatory since 1958, on data from close to the coast of Antarctica (Etheridge et al., 1996) and future predictions from NOAA (Raes et al., 2013).

2.2. Crop simulation model

A simulation model, hereafter referred to as AdaptaOlive, based on experimental data generated by previous studies, has been developed to obtain yield, irrigation requirement and economic projections for traditional olive orchards under several climate and management scenarios.

The core of the simulation model is olive yield assessment based on olive transpiration estimation. Olive transpiration (T) is assessed using the experimental procedure developed by Orgaz et al. (2006) for determining T under optimal irrigation and baseline conditions ($T_{o\text{-}B}$), based on the fraction of intercepted diffuse radiation. To determine T under optimal irrigation and future climate conditions, $T_{o\text{-}B}$ is reduced by a term, named R_{gc}, representing the reduction in canopy conductance when atmospheric CO_2 increases. This term was estimated by Field et al. (1995) for tree species based on experimental data and reads as follows:

$$R_{gc} = 0.0665 \cdot [CO_2] - 22.934 \quad (1)$$

where $[CO_2]$ is the atmospheric CO_2 concentration in parts per million (ppm). This assumption was validated by Drake et al. (1997) based on FACE experiments, and by Moriana et al. (2002), Villalobos and Fereres (2004) and Viola et al. (2014) specifically for the olive crop.

Transpiration efficiency (TE) is defined as the ratio between net assimilation and transpiration and depends on the ambient (C_a) and inner leaf (C_i) CO_2 concentration and on vapor pressure deficit (VPD), as defined by Beer et al. (2009). In this study, C_a was determined for baseline and future periods by measurements and projections from NOAA (Raes et al., 2013). A constant value of 0.69 for C_i/C_a was used, as measured by Tognetti et al. (2002). Similarly, Villalobos et al. (2012) indicated an overall improvement in water use efficiency in olive trees under water deficit, and several authors have reported a reduction in C_i/C_a (and thus an increase in TE) when water stress increased (Brodribb, 1996; Bacelar et al., 2007; Gómez del Campo, 2013; López-Bernal et al., 2015). As specific functions for olive were not available, a new approach was developed for the AdaptaOlive model. Thus, the new function defined a reduction factor, termed $F_{Ci/Ca}$, for modifying C_i/C_a

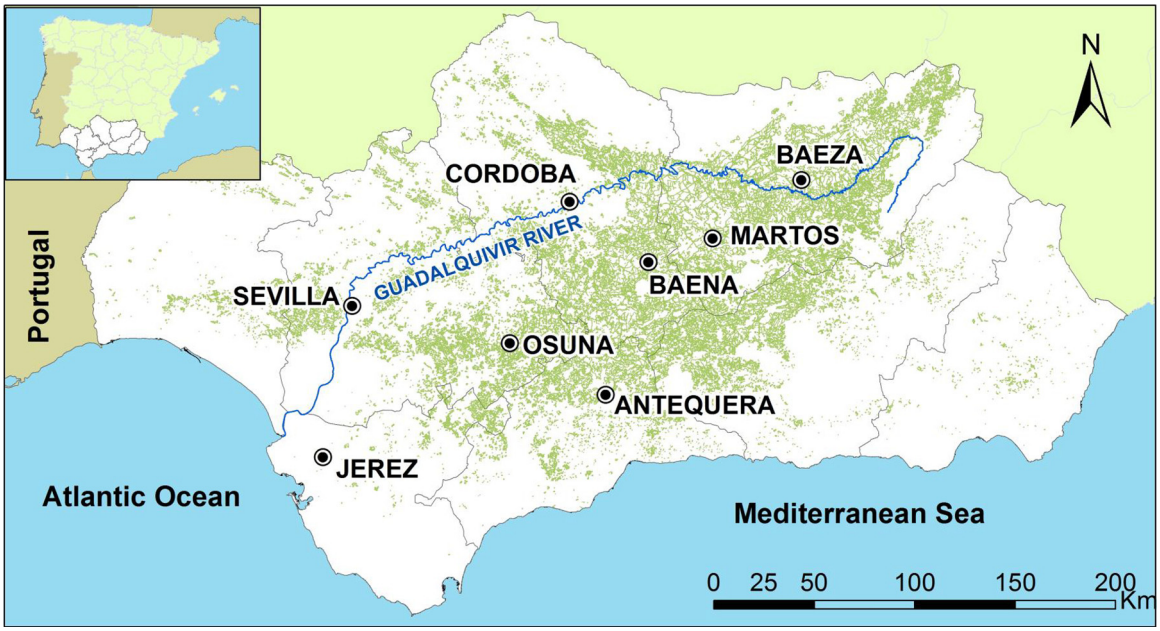

Fig. 1. Map of the region of Andalusia indicating the eight representative locations considered in the study. Current olive-cultivated areas are shown in green.

using a polynomial curve based on the ratio of seasonal transpiration under the analyzed and non-stressed conditions (R_T), generating an increase in TE when stomatal closure caused by crop water stress occurred. The proposed function was obtained from experimental data for different deficit irrigation strategies in olive described in Bacelar et al. (2007), with values of R_T ranging from 0.3 to 1, and reads as:

$$F_{Ci/Ca} = -0.309 \cdot R_T^2 + 0.773 \cdot R_T + 0.536 \quad (2)$$

Potential oil yield for baseline (B) weather conditions ($Y_{max\text{-}B}$) was calculated following the simplified equation defined by Villalobos et al. (2006) based on annual incoming photosynthetically active radiation (PAR), radiation use efficiency (RUE, equal to 0.17, following Villalobos et al., 2006), and the fraction of PAR intercepted by the canopy (equal to 0.45, following Monteith, 1965, and Meek et al., 1984). Based on $Y_{max\text{-}B}$, potential oil yield for any year t ($Y_{max\text{-}t}$) can be determined using a change factor calculated as:

$$Y_{max-t} = Y_{max-B} \cdot \frac{T_t}{T_B} \cdot \frac{TE_t}{TE_B} \cdot \frac{HI_t}{HI_B} \quad (3)$$

where HI_t and HI_B are the harvest index, defined as the ratio between olive oil yield and the annual increase in total biomass, t is the analyzed year, and B the baseline period. In this study, the ratio HI_t/HI_B was taken as equal to 1 for any year analyzed as there are no available projections of future changes in this ratio.

Finally, to calculate oil yield under water stressed scenarios (Y_w), a function proposed by Mesa-Jurado et al. (2010), based on Moriana et al. (2003) was taken:

$$Y_w = Y_{max} \cdot [0.9558 \cdot R_T^2 + 1.9646 \cdot R_T - 0.088] \quad (4)$$

where R_T is the ratio of seasonal transpiration under a baseline and non-stressed scenario. The reduction in T caused by water stress was computed following Allen et al. (1998).

This simulated yield could be affected in addition by many factors, such as lack of chilling hours, water stress during flowering and/or ripening, heat stress during flowering or the impact of alternate bearing. Unfortunately, information is available for very few of these factors. Only the impact of water stress during flowering has been analyzed in detail (Moriana et al., 2003; Rapoport et al., 2012), demonstrating that water deficit during inflorescence development reduces inflorescence and flower number, and ovule development. Using experimental data collected by Rapoport et al. (2012), a linear function was developed for calculating a reduction factor (F_R) of Y_w, ranging from 0 to 1, to determine the olive oil yield (Y_c) when accounting for water stress during the flowering stage (R0C strategy). This function reads as:

$$\begin{cases} F_R = 1.7364 \cdot k_{s-flo} - 0.2155 & k_{s-flo} \le 0.7 \\ F_R = 1 & k_{s-flo} > 0.7 \end{cases} \quad (5)$$

where $k_{s\text{-}flo}$ is a coefficient describing the intensity of the water stress during the flowering stage.

To identify the flowering date for each location, period and cultivar, a phenological model developed by Gabaldón-Leal et al. (2017) was used. In that study, flowering failure related to insufficient chilling hours was only found for coastal areas of Andalusia (outside the traditional olive area), with the results showing a very low percentage of occurrence, and a high level of uncertainty (Gabaldón-Leal et al., 2017); therefore, this kind of flowering failure was not considered in this study.

Finally, irrigation water requirements were estimated by means of a water balance approach. For full irrigation strategy (R2), irrigation supply was managed in such a way that the soil water deficit did not exceed 75% of the water holding capacity (Orgaz and Fereres, 2004) during the whole crop cycle. For the regulated deficit irrigation strategy (R1), it was only during flowering and ripening stages that irrigation was applied under the same rules as for R2.

Once yield and irrigation requirements had been estimated, net margin (NM), water productivity (WP) and irrigation water productivity (IWP) were calculated. NM computes incomes and outcomes based on the agro-economical parameterization carried out by Mesa-Jurado et al. (2010) for a typical olive orchard located in Andalusia. The main parameters were the olive price (p) and the irrigation water cost (k_w) with values equal to 0.52 € kg^{-1} and 0.26 € m^{-3}, respectively, based on averaged data compiled by Mesa-Jurado et al. (2010) for the period 2005–2008, but valid for current conditions. The ratio between oil and olive fruit yield varies with water supply and the harvesting date but in this study, it was taken as constant for the whole period and equal to 0.22 (Mesa-Jurado et al., 2010). Water productivity (WP) was calculated as the ratio between oil yield and the sum of rainfall and irrigation supply, and irrigation water productivity (IWP) was defined as the ratio between the increase in yield caused by irrigation and the irrigation supply.

Fig. 2 shows a flowchart depicting the integration of the approaches described above.

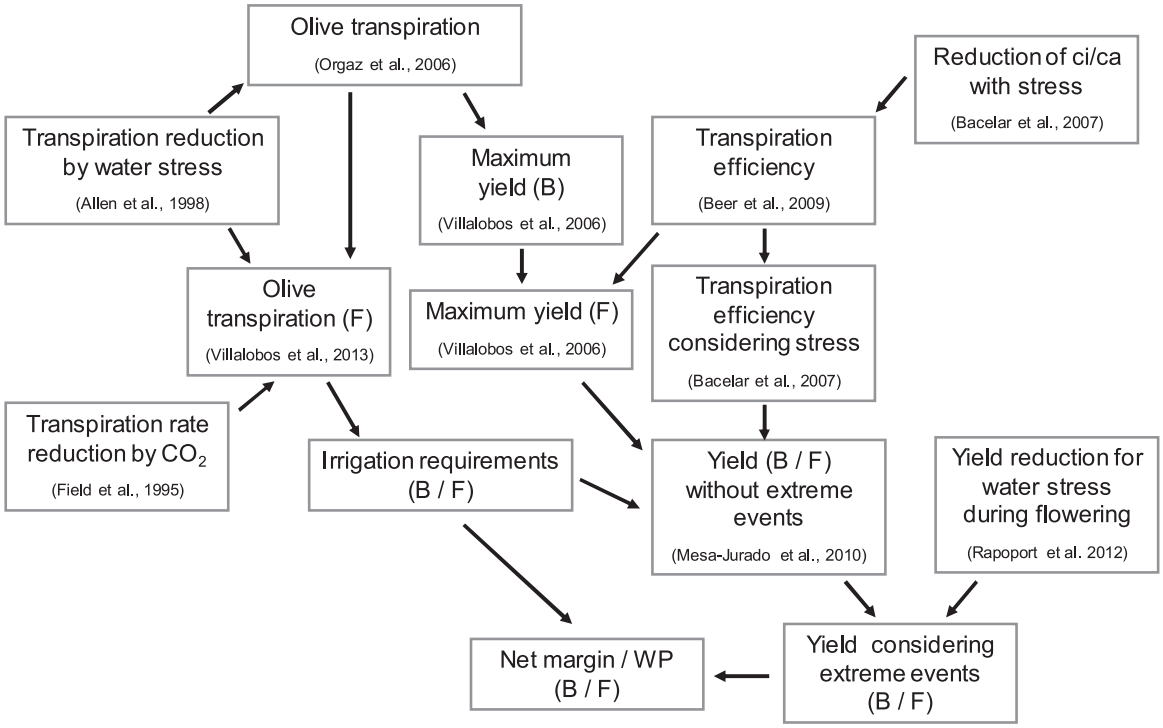

Fig. 2. Flow-chart with the approaches integrated in the AdaptaOlive model and the interaction between them. The periods analyzed using each approach (baseline, B and/or future, F) are also shown.

2.3. Agronomic scenarios

The study focused on a representative olive orchard with characteristics typical of the modern orchards in the region of Andalusia. Tree density was 250 olive trees per hectare with a 5 m canopy diameter (around 50% of soil cover) in a field with 10% slope, soil with water holding capacity of 150 mm m^{-1} and a depth of 1.2 m. For this representative olive orchard, simulations were carried out for different irrigation strategies, olive genotypes, climate projections, periods and locations.

Three irrigation strategies were considered: rainfed (R0); regulated deficit irrigation, providing irrigation only during flowering and ripening stages (R1); and full irrigation, avoiding water stress in any period during the crop cycle (R2). Five olive genotypes were evaluated: 'Arbequina', 'Picual', 'GM22', 'FV18' and 'Chiquitita'. 'Arbequina' and 'Picual' are traditional Spanish cultivars, originating from northern and southern Spain, respectively. 'GM22' and 'FV18' are wild olive genotypes that belong to the *Olea europaea* subsp. *guanchica* and are indigenous to the subtropical climate of the Canary Islands, which have annual mean temperatures of 20 °C and a relatively small intra-annual temperature oscillation. These two wild trees were included in this study to assess the potential behavior of late flowering cultivars. Finally, 'Chiquitita' is a new cultivar obtained by systematic breeding from progeny of the 'Arbequina' x 'Picual' cross (Rallo et al., 2008).

The evaluation of olive response under future climate conditions in terms of transpiration (T), transpiration efficiency (TE), phenology, water stress, net margin (NM), water productivity (WP) and irrigation water productivity (IWP), was based on the olive orchard described above, located in the Baeza area (Fig. 1), with the olive cultivar 'Picual'. Weather data were sourced from the ensemble member closest to the average of the ENS-SP ensemble (the DMI-BCM outputs, Table 1). This agronomic scenario is hereafter referred to as DMIB-Pic-BA. In addition, a spatial and genotype analysis of the impact of future climate conditions on olive yield, irrigation requirements, and economic projections with DMI-BCM climate projection was carried out. In a second step, the same orchard was analyzed to examine how the uncertainty from climate projections propagate through the main components of the olive crop. For this task, the entire ensemble of climate projections ENS-SP described in Section 2.1. was considered.

Table 1
Change in simulated rainfall, mean temperature and reference evapotranspiration (ET_o) during near (NF) and far future (FF) periods compared with baseline (B) period for the ENS-SP ensemble mean and for each climate projection considered, for a representative olive orchard in the Baeza area.

Climate projection	Rainfall		Mean Temperature		ET_o	
	NF vs. B (%)	FF vs. B (%)	NF vs. B (°C)	FF vs. B (°C)	NF vs. B (%)	FF vs. B (%)
Ensemble mean (ENS-SP)	−7.5	−23.5	1.4	3.5	4.8	12.1
DMI_ARPEGE	−4.4	−27.2	1.5	2.8	5.6	3.7
DMI_BCM	−7.6	−22.0	0.9	3.3	4.2	13.3
ETHZ	−10.7	−20.5	1.7	3.3	4.2	9.7
C4I_HadCM3Q16	−10.1	−29.8	1.8	4.7	6.3	17.8
HC_HadCM3Q0	−12.3	−16.9	1.8	3.7	6.4	13.7
KNMI	−12.1	−29.3	1.2	3.9	5.4	15.4
MPI	−9.8	−29.3	1.3	4.2	4.6	13.5
R_CNRM_ARPEGE	−4.2	−26.5	1.6	3.6	3.8	10.8
SMHI_BCM	−7.4	−17.3	0.8	2.4	3.6	9.8
SMHI_ECHAM5	−9.6	−29.1	1.0	3.3	4.3	13.8
SMHI_HadCM3Q3	5.8	−9.9	1.3	3.0	4.4	12.0

3. Results

3.1. Olive response to climate change

The results of the AdaptaOlive model applied in a representative olive orchard cultivated in the Baeza area with 'Picual' cultivar (Table 1), and under the DMIB-Pic-BA scenario indicate that olive crop transpiration (T) would be reduced in NF and FF periods, compared with the B period, with the most severe reductions under rainfed conditions (decreases of around 9 and 22% for NF and FF, respectively;

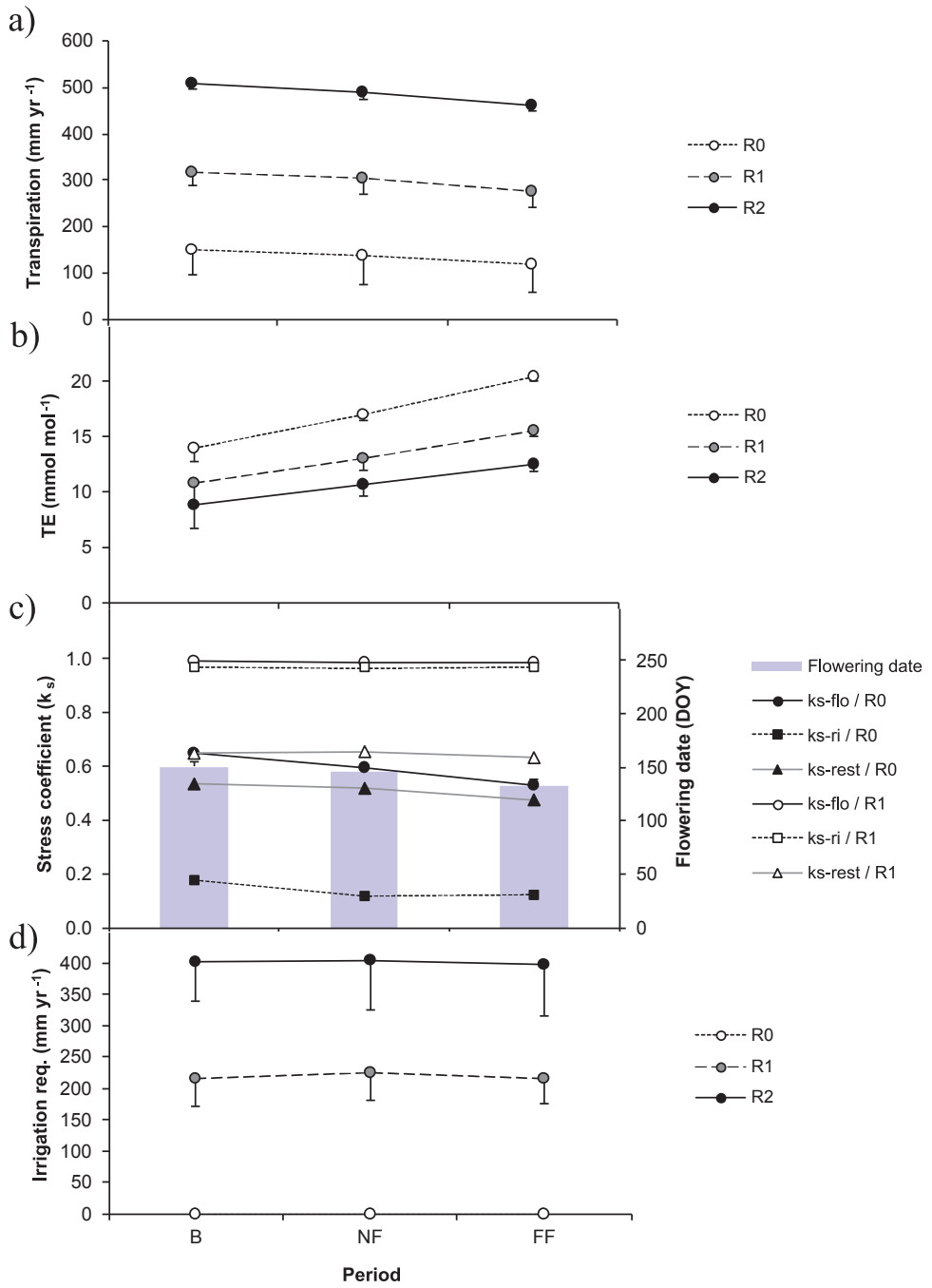

Fig. 3. Transpiration (a), transpiration efficiency (b), stress coefficient (c) and irrigation requirements (d), for rainfed (R0), regulated deficit irrigation (R1) and full irrigation (R2) for baseline (B), near future (NF) and far future (FF) periods under the DMIB-Pic-BA agronomic scenario. Vertical lines indicate interannual standard deviation.

Fig. 3a). The opposite was found for transpiration efficiency (TE), with increases in NF and FF periods (Fig. 3b). Thus, TE increased by around 22 and 47% under rainfed conditions (R0) for NF and FF, respectively (Fig. 3b). The AdaptaOlive model showed that simulated crop water stress during flowering was reduced by the advance in the flowering date (from DOY 151 in B to DOY 146 and 133 for NF and FF periods, respectively, regardless of the irrigation treatment) and amplified by the reduction in rainfall (Table 1). The combination of these two factors resulted in increased water stress during flowering (WSF) under rainfed conditions: average $k_{s\text{-}flo}$ decreased by around 8 and 19% from B to NF and FF periods, respectively (Fig. 3c).

As result of these changes, under rainfed conditions simulated olive oil yield (Y_c) from the DMIB-Pic-BA projection increased by around 4% in the NF period, and decreased by around 1.5% in the FF period, compared with B (Fig. 4a). Similar results were found for net margin (NM_c), with increases of 6.5% for NF and decreases of around 2% for FF compared with the B period (Fig. 4b). The impact of water stress during flowering on yield (Y_w *vs.* Y_c) generated reductions of 16.7, 20.8 and 26.0%, for B, NF and FF, respectively, while the corresponding decreases in net margin (NM_w *vs.* NM_c) were 22.7, 27.4 and 34.2%. Finally, WP_c showed increases of around 7 and 33% for NF and FF, respectively, compared with the B period (Fig. 4c).

Similarly, under irrigation, mean Y_c increases of around 16% and 27% were found for NF and FF, respectively (Fig. 4a), and mean NM_c increases of 24 and 41% for NF and FF, respectively (Fig. 4b). In both cases, increases were higher for the R2 strategy. Irrigation requirements

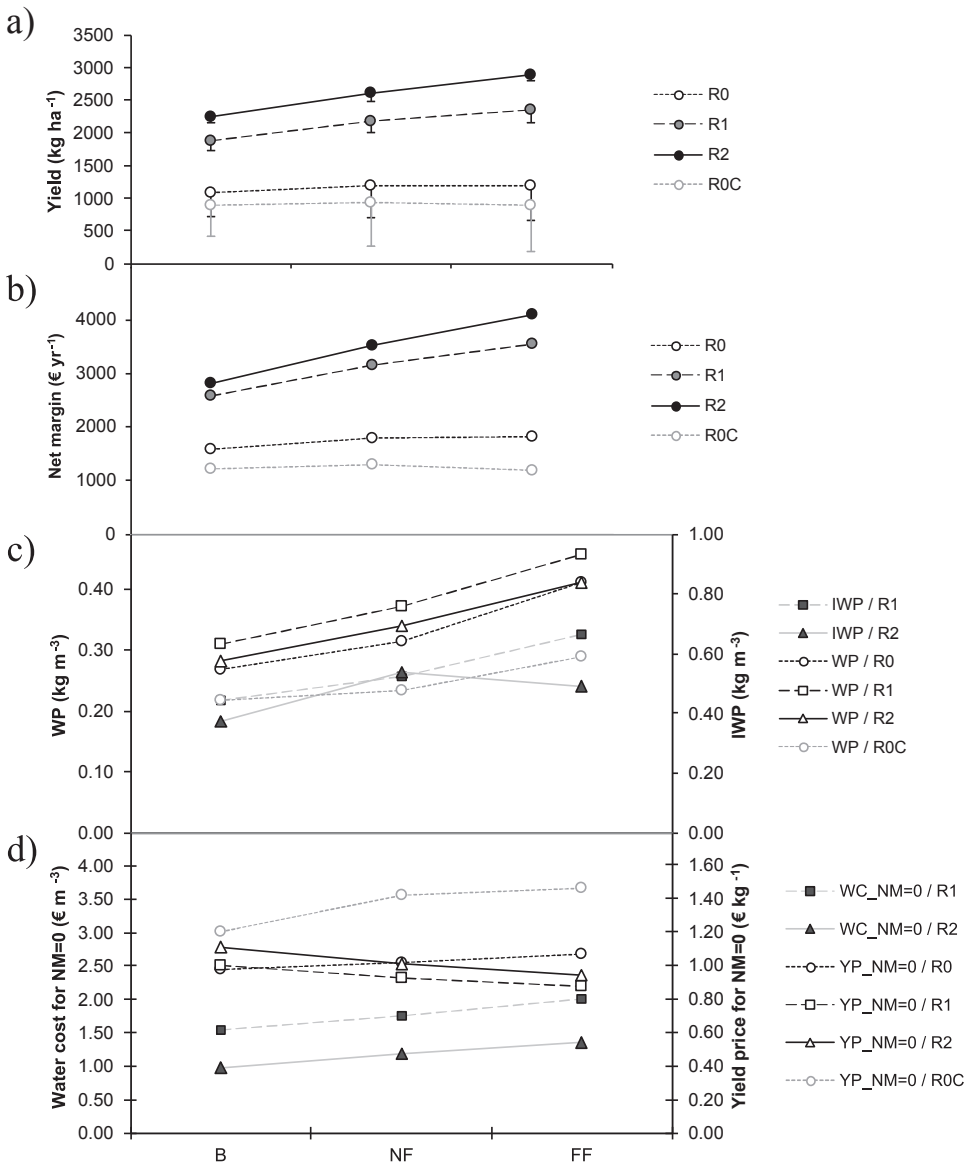

Fig. 4. Yield (a), net margin (b), water productivity and irrigation water productivity (c) and water cost (WC_NM = 0) and yield price (YP_NM = 0) thresholds for NM = 0 (d), for rainfed conditions accounting for (R0C) and not accounting for water stress during flowering (R0), regulated deficit irrigation (R1) and full irrigation (R2), for baseline (B), near future (NF) and far future (FF) periods under the DMIB-Pic-BA agronomic scenario. Vertical lines indicate interannual standard deviation.

(IR) derived from the DMIB-Pic-BA agronomic scenario were hardly affected in the future periods. Considering regulated deficit irrigation, IR were 216, 225 and 215 mm for B, NF and FF, respectively, and considering full irrigation, the corresponding values were 402, 403 and 397 mm for B, NF and FF periods, respectively (Fig. 4d).

WP_c increased in future periods with mean values of around 20 and 47% for NF and FF, respectively. IWP_c with R1 increased for NF and FF compared with B (by 19 and 50%, respectively), but this trend changed for R2, with the highest increases for the NF period (45%; Fig. 4c). Water cost threshold for NM = 0 (WC_NM = 0) during the B period showed high values of around 1.5 and 1.0 € m^{-3} for R1 and R2, respectively (Fig. 4d). These values increased by around 14 and 20% for NF, and by around 30 and 38% for the FF period. Finally, for oil yield price threshold for NM = 0 (YP_NM = 0) during the B period, the values were low enough to ensure a positive net margin with values equal to 1.2, 1.0 and 1.1 € kg^{-1} for R0C, R1 and R2, respectively, and with even lower values for future periods under irrigated strategies (Fig. 4d).

3.2. Inter-annual variability of the impacts

Graphing the simulated annual yield *vs.* the crop transpiration reveals the inter-annual variability in yield and allows the identification of yield functions, including the impact of water stress during flowering, depending on the period and irrigation availability (e.g. in Fig. 5 for the DMIB-Pic-BA climate projection). Yield values can be grouped depending on the period and irrigation strategy, exhibiting a higher inter-annual variability for NF and FF compared with the B period (e.g. for the R0C strategy, inter-annual coefficients of variation, CVs, were equal to 52.3, 71.4 and 78.3%, for B, NF and FF, respectively; Figs. 4a and 5). Similarly, inter-annual variability for yield was affected by the irrigation strategy considered, dramatically decreasing with the irrigation supply (Figs. 4a and 5). Thus, CVs for yield during the B period were equal to 52, 8 and 4% for R0C, R1 and R2 strategies, respectively (Figs. 4a and 5). Finally, accounting for water stress during flowering increased the inter-annual variability of yield, with CVs equal to 32 and 52% for R0 and R0C, respectively (Figs. 4a and 5).

For net margin (NM_c) a high inter-annual variability was found,

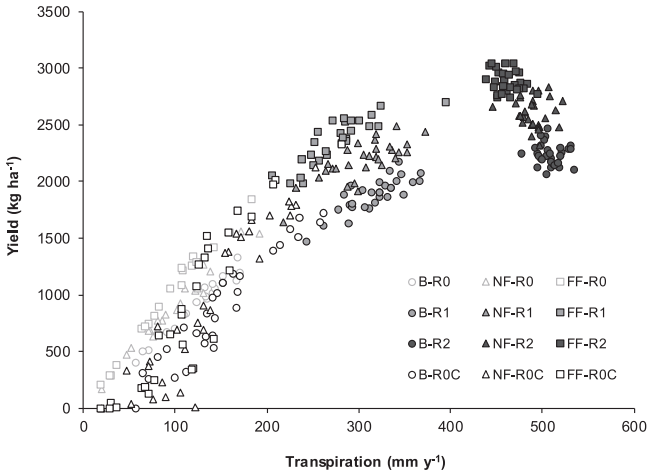

Fig. 5. Correlation between annual values of yield and transpiration (T) sorted by period (baseline, B, near future, NF, and far future, FF) and irrigation strategy (R0C, R0, R1 and R2) for DMIB-Pic-BA agronomic scenario.

especially under rainfed conditions, with differences between the yearly minimum and maximum NM_c values of 3420, 4231 and 4638 € ha^{-1}, for B, NF and FF periods, respectively (Fig. 6). When irrigation was applied, the differences were much lower: with R2, the maximum differences between years were 1196, 1191 and 1021 € ha^{-1} for B, NF and FF, respectively (Fig. 6).

The analysis of the inter-annual variability permitted the assessment of the probability of occurrence that the net margin was negative ($NM_c < 0$). Thus, considering rainfed conditions and an olive oil price of 2.36 € kg^{-1}, the probability of occurrence of $NM_c < 0$ increases in the future, from 10% in B to 23.3 and 28.6% for NF and FF, respectively (Fig. 6). Under irrigation, the trend is the opposite: with the current water costs (0.26 € m^{-3}) and olive oil price (2.36 € kg^{-1}), no years with $NM_c < 0$ are predicted. When increasing the water cost to 1.2 € m^{-3}, which is feasible when non-conventional water resources such as reclaimed or desalinated water are considered, the probability of occurrence of years with $NM_c < 0$ decreases in the future. Thus, for R1, the probability of occurrence of $NM_c < 0$ decreased from 20% in B to 6.7 and 3.6% for NF and FF, respectively, and with R2 from 86.7% in B to 56.7 and 35.7% for NF and FF, respectively. Finally, with current water costs (0.26 € m^{-3}) and low oil yield prices (1.5 € kg^{-1}) the probability of occurrence of $NM_c < 0$ for rainfed conditions was equal to 20, 33.3 and 35.7% for B, NF and FF, respectively. However, for R1 and R2 strategies, the probability of occurrence of $NM < 0$ was negligible, even for low oil prices.

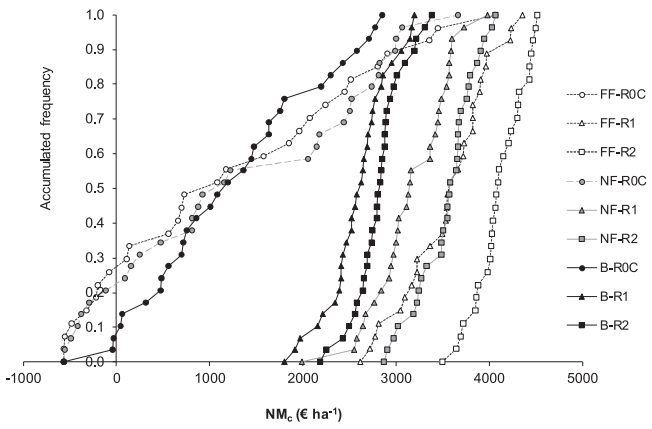

Fig. 6. Interannual variability of net margin (NM_c) considering current water cost and olive oil prices for baseline (B), near future (NF) and far future (FF) periods, and R0C, R1 and R2 irrigation strategies, for DMIB-Pic-BA agronomic scenario.

3.3. Spread of olive response to climate change

To evaluate how uncertainty from the ensemble of climate projections propagates through impact projections, the AdaptaOlive model was applied to the same olive orchard in the Baeza area, and all ensemble members of ENS-SP. The average advance in flowering date was around 6 and 18 days for NF and FF periods, respectively, ranging from 4 to 12 days for NF and from 13 to 25 days for FF (Table 2). When evaluating olive oil yield under rainfed conditions, average increases of 14.8 and 7.1% for NF and FF periods were found in comparison with the B period (Table 2), ranging from −4.0 to +50.2% for NF and from −14.1 to +44.2% for FF (Table 2 and Fig. 7). Under irrigation regimes, oil yield increases varied according to the analyzed period and irrigation strategy (for NF, 12.6 and 14.7% for R1 and R2, respectively, and for FF, 21.5 and 28.9% for R1 and R2, respectively). The ensemble spread in oil yield decreased with the amount of water applied (e.g. for FF, the spread was 9.9–31.5%, and 24.0–35.7%, for R1 and R2, respectively). Likewise, both net margin (NM_c) and water productivity (WP_c) increased from B to NF and FF, with a substantial spread in projections, mainly under rainfed conditions (Tables 2 and 3).

The behavior described is a consequence of changes in transpiration (T), transpiration efficiency (TE) and stress coefficients ($k_{s\text{-}flo}$) during flowering for NF and FF periods compared with B. Thus, under rainfed conditions, TE increased around by 20 and 51% for NF and FF periods, respectively, with a slightly lower increase under irrigation (Table 4), and with a moderate spread in projections (e.g. the spread for FF ranged from 41 to 63% for rainfed conditions; Table 4). There was a reduction in transpiration (T) for future periods, especially under rainfed conditions (8 and 28% for NF and FF, respectively) with a large spread in projections (reductions of between 6 and 39% for rainfed conditions in FF; Table 4). Finally, $k_{s\text{-}flo}$ registered increases of 4% in NF and reductions of 7% in FF under rainfed conditions, but it also showed a large spread (e.g. $k_{s\text{-}flo}$ values for FF ranged from increases of 12% to reductions of 19%; Table 4).

For the baseline period (B), water stress during flowering under rainfed conditions generated average reductions in yield of 19.8% (varying between 11.9 and 34.0% depending on the ensemble projection), in net margin of 25.9% (between 15.1 and 45.6%), and in water productivity of 24.7% (between 16.0 and 45.2%). For future conditions, similar average reductions (e.g. for FF, 20.1, 26.0 and 26.4% for yield, net margin and water productivity, respectively) and spread were found (Table 1S).

Average irrigation requirements were slightly reduced for R1 and R2 irrigation strategies when NF and FF periods were compared with B (Table 3). In both cases, there was significant ensemble spread (e.g. in FF for R1, values ranged between −14.9% and +4.5%, and for R2, between −10.7% and +8.5%; Table 3). Similarly, due to yield increases and irrigation decreases, irrigation water productivity increased for future periods compared with B, with mean increases for FF equal to 46.1 and 17.3% for R1 and R2, respectively, and with a large spread in projections within the ensemble (Table 3).

3.4. Spatial variability of the impacts

Extending the study to the whole region of Andalusia (Fig. 1), high spatial climate variability was detected. Specifically considering the DMI-BCM climate projection for Andalusia, annual rainfall ranged spatially from 105 to 924 mm, and from 80 to 648 mm, for B and FF periods, respectively, while average temperature ranged between 11.1 and 18.7 °C, and 14.3 and 21.7 °C, for B and FF periods, respectively. Changes in temperature and precipitation for NF were between those reported for B and FF. As a result of the differences in the temperature pattern, the flowering date for 'Picual' cultivar in the B period ranged spatially across Andalusia from 128 DOY to 180 DOY, and from 116 DOY to 156 DOY for the FF period. Similarly, simulated Y_c considering the scenario described in Section 2.3. showed high spatial variability

Table 2
Change in simulated flowering date, yield (Y_c) and net margin (NM_c) during near future (NF) and far future (FF) periods compared with baseline (B) period for the ensemble mean and for each climate projection considered, for a representative olive orchard with 'Picual' cultivar in the Baeza area. R0C, R1 and R2 are rainfed, deficit irrigation and full irrigation strategies, respectively. Negative values in flowering date indicate an advance in flowering (in days) for the FF period compared with the B period.

	Climate projection	Flowering date (days)	Y_c (%)			NM_c (%)		
			R0	R1	R2	R0	R1	R2
NF vs. B	Ensemble mean (ENS-SP)	−6.2	14.8	12.6	14.7	21.4	18.4	22.2
	DMI_ARPEGE	−5.5	33.6	13.6	15.4	54.7	21.0	24.3
	DMI_BCM	−4.8	4.4	15.8	16.3	6.5	22.1	25.7
	ETHZ	−7.4	1.1	8.1	12.2	1.6	13.2	19.1
	C4I_HadCM3Q16	−11.5	12.0	7.8	12.0	18.0	12.2	16.9
	HC_HadCM3Q0	−9.0	5.7	6.8	11.1	7.7	10.0	15.1
	KNMI	−4.7	−4.0	15.1	17.7	−5.7	21.0	25.5
	MPI	−4.5	11.3	16.6	18.7	16.4	24.7	28.6
	R_CNRM_ARPEGE	−6.5	28.1	10.0	11.8	36.9	15.0	17.0
	SMHI_BCM	−4.5	17.3	13.2	14.3	24.8	18.1	22.1
	SMHI_ECHAM5	−3.9	2.9	14.4	16.7	3.8	20.0	23.7
	SMHI_HadCM3Q3	−6.1	50.2	16.8	15.8	71.1	25.3	25.9
FF vs. B	Ensemble mean (ENS-SP)	−17.5	7.1	21.5	28.9	10.5	31.3	44.0
	DMI_ARPEGE	−13.4	27.1	22.6	29.9	44.0	35.1	49.9
	DMI_BCM	−18.0	−1.5	25.2	28.8	−2.1	36.7	46.1
	ETHZ	−17.2	5.4	21.4	30.2	7.7	33.2	48.4
	C4I_HadCM3Q16	−25.4	−7.2	9.9	22.2	−10.8	14.6	30.5
	HC_HadCM3Q0	−21.4	5.9	19.1	27.2	7.9	28.1	39.7
	KNMI	−17.7	−3.8	22.8	32.3	−5.3	32.1	47.9
	MPI	−18.4	1.5	25.0	35.7	2.2	36.8	54.0
	R_CNRM_ARPEGE	−16.9	15.7	17.3	24.0	20.7	24.7	34.5
	SMHI_BCM	−12.5	4.9	20.8	26.7	7.0	30.0	41.3
	SMHI_ECHAM5	−16.7	−14.1	20.4	29.0	−18.5	27.8	41.2
	SMHI_HadCM3Q3	−14.6	44.2	31.5	32.1	62.6	45.1	50.1

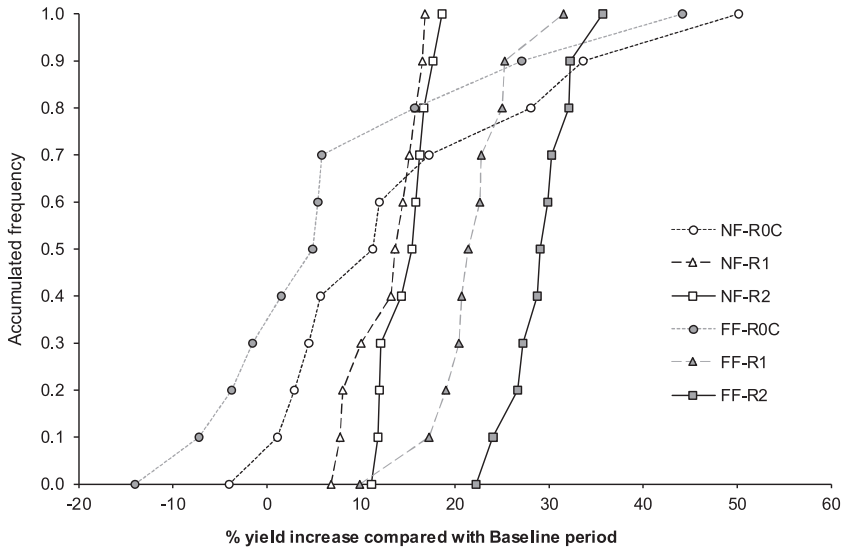

Fig. 7. Cumulative frequency of the ensemble mean yield (Y_c) increase (as a percentage) for near future (NF) and far future (FF) periods compared with baseline (B), for 3 irrigation supply strategies (R0C, R1 and R2) in the Baeza area with 'Picual' cultivar.

within Andalusia, ranging from 23 to 1861 kg ha^{-1} for B, from 41 to 2163 kg ha^{-1} for NF, and from 32 to 2163 kg ha^{-1} for FF (Fig. 8a); the areas with the highest values are in the southwest, and the lowest in the east of the region (Fig. 9).

When analyzing the cumulative frequency curves of Y_c and NM_c over Andalusia, the highest spatial variability was found under rainfed conditions (Figs. 1Sa and 1Sb). For IR, cumulative frequency curves showed a very similar spatial pattern for the three periods, with high spatial variability, but small differences between R1 and R2 (Fig. 1Sc). Thus, IR ranged from 80 to 290 mm and from 100 to 602 mm, for R1 and R2, respectively, with only small variations between the baseline and future periods (Fig. 8b). The areas with the highest requirements were in the east of the region and in the Guadalquivir Valley, while the areas with the lowest requirements were in hilly areas in the north and south (Figs. 8b and 9).

Analyzing each location under irrigated conditions, simulated changes in Y_c, NM_c and WP_c for NF and FF compared with the B period were similar for all the locations selected (Table 5). However, changes in IR ranged from increases of around 10% for areas such as the Jerez area, to limited changes for the Baeza area (Tables 5 and 2S). Under rainfed conditions, the Y_c pattern varied between locations and periods, with an increase in Y_c in NF in all the analyzed locations (Table 2S), but with most locations registering a decrease in FF (Table 5). One cause of this pattern was the difference in water stress during flowering (WSF)

Table 3
Change in simulated irrigation requirements (IR), water productivity (WP_c) and irrigation water productivity (IWP_c) during far future (FF) period compared with baseline (B) period for the ensemble mean and for each climate projection considered, for a representative olive orchard with 'Picual' cultivar in the Baeza area. R0C, R1 and R2 are rainfed, deficit irrigation and full irrigation strategies, respectively.

	Climate projection	Irrigation (%)		WP (%)			IWP (%)	
		R1	R2	R0	R1	R2	R1	R2
NF vs. B	Ensemble mean (ENS-SP)	−4.1	0.3	20.8	19.8	18.9	16.8	30.4
	DMI_ARPEGE	−8.4	−1.6	40.2	21.8	19.0	13.5	30.6
	DMI_BCM	4.3	0.3	6.7	19.8	20.4	19.0	44.7
	ETHZ	−7.4	−0.2	10.9	18.9	18.4	24.9	38.2
	C4I_HadCM3Q16	−6.9	2.7	17.2	17.5	15.7	12.5	28.5
	HC_HadCM3Q0	−4.7	3.6	13.7	18.8	16.4	13.2	53.4
	KNMI	4.5	6.7	3.7	21.5	21.0	31.6	41.8
	MPI	−2.5	2.7	20.5	24.9	23.3	24.6	31.9
	R_CNRM_ARPEGE	−12.0	−1.8	36.3	17.9	15.5	4.3	16.4
	SMHI_BCM	0.9	−2.6	23.6	17.0	19.6	12.0	26.5
	SMHI_ECHAM5	−1.9	2.2	15.7	22.5	21.3	31.0	26.7
	SMHI_HadCM3Q3	−10.9	−8.8	40.5	16.8	17.1	−1.5	−4.3
FF vs. B	Ensemble mean (ENS-SP)	−6.2	−0.5	36.2	46.9	46.6	46.1	17.3
	DMI_ARPEGE	−14.9	−10.7	78.6	58.9	58.1	44.7	−15.3
	DMI_BCM	−0.5	−1.2	32.8	47.3	46.0	50.2	31.8
	ETHZ	−11.1	−2.6	37.9	48.8	47.6	53.4	12.7
	C4I_HadCM3Q16	−4.6	7.3	19.4	36.1	35.2	27.9	−8.1
	HC_HadCM3Q0	−12.9	−0.1	30.1	43.6	40.1	50.9	16.3
	KNMI	4.5	8.5	17.7	49.1	49.1	50.3	36.0
	MPI	−1.6	6.7	29.9	56.3	54.5	51.0	34.3
	R_CNRM_ARPEGE	−12.1	−3.3	56.5	48.4	46.2	39.8	5.1
	SMHI_BCM	−6.5	−5.4	26.4	37.4	42.3	48.2	16.6
	SMHI_ECHAM5	0.0	4.4	14.5	48.1	47.7	66.5	32.2
	SMHI_HadCM3Q3	−8.1	−9.2	54.5	41.7	45.6	24.2	28.5

between locations. Thus, in the Baeza area, WSF reduced Y_c (compared with Y_w) by around 17, 21 and 26%, for B, NF and FF, respectively, but in other areas such as Córdoba, the corresponding reduction was only 3, 4 and 12% (Table 6). NM_c followed the same spatial pattern as Y_c; e.g. changes in FF compared with the B period, ranging from reductions of around 12% for the Baena and Martos areas to increases of 5% for the Seville area (Table 5).

3.5. Variability among olive genotypes

The simulated flowering date in the Baeza area using the DMI_BCM climate projection was very similar for the genotypes under study, except for 'GM22', which showed a consistent delay of around 21 days on average across periods (B, NF, FF) compared with the rest of the genotypes (Table 7). Due to this delayed flowering date, under regulated deficit irrigation strategy (R1), the 'GM22' genotype registered increases in IR of around 19, 12.5 and 10.5%, for B, NF and FF, respectively; very limited increases in oil yield (3.8, 3.6 and 1.9%); and negligible changes in WP_c and IWP_c, compared with the rest of the genotypes (Table 7). Differences between other genotypes and 'GM22' in Y_c, NM_c, IR, WP_c and IWP_c were smaller for the FF period than the B period (Table 7).

Under rainfed conditions, Y_c for 'GM22' in the Córdoba area was 6, 4 and 1% lower than the rest of the genotypes under study, for B, NF and FF, respectively, and in drier areas such as the Baeza area, the reduction in yield was 17, 10 and 7% for B, NF and FF, respectively (Fig. 10). For NM_c greater reductions were detected for 'GM22' than the rest of the genotypes; in the Córdoba area, NM_c for 'GM22' was lower than for the rest of the genotypes by around 7, 5 and 1% for B, NF and FF, respectively, and in the Baeza area around 25, 15 and 10%. As with the results under irrigation in the Baeza area, the differences between genotypes in Y_c and NM_c were smaller for the FF period than the B period.

Table 4
Mean, standard deviation (SD), maximum and minimum changes in transpiration efficiency (TE), transpiration (T), water stress during flowering ($k_{s\text{-}flo}$), water cost for NM = 0 (PA_NM0) and yield price for NM = 0 (PK_NM0) considering 11 climate models for rainfed (R0), regulated deficit irrigation (R1) and full irrigation (R2).

IS		TE		T		$k_{s\text{-}flo}$		PA_NM0		PK_NM0	
		NF vs. B (%)	FF vs. B (%)	NF vs. B (%)	FF vs. B (%)	NF vs. B (%)	FF vs. B (%)	NF vs. B (%)	FF vs. B (%)	NF vs. B (%)	FF vs. B (%)
R0C	Mean	20.1	50.7	−8.2	−27.9	4.3	−6.8			4.3	19.5
	SD	3.9	6.6	8.1	8.6	9.8	10.4			13.1	29.2
	Max	25.9	62.6	13.9	−6.0	21.9	12.4			24.6	87.9
	Min	14.6	40.8	−16.5	−38.7	−8.5	−18.7			−22.7	−16.7
R1	Mean	20.1	50.0	−6.2	−18.8			21.2	35.9	−7.5	−11.9
	SD	2.4	6.3	2.2	3.8			7.1	12.1	1.7	2.6
	Max	24.3	62.3	−1.1	−10.5			37.0	54.9	−4.7	−6.3
	Min	16.1	39.9	−9.6	−24.3			11.8	16.9	−10.9	−16.1
R2	Mean	18.5	43.7	−3.1	−10.1			16.3	34.3	−8.1	−14.5
	SD	2.9	6.4	0.8	2.7			6.1	10.3	1.8	2.6
	Max	22.7	56.2	−1.7	−6.0			32.6	53.9	−5.0	−9.0
	Min	13.0	30.1	−4.3	−16.8			9.6	16.1	−11.6	−18.7

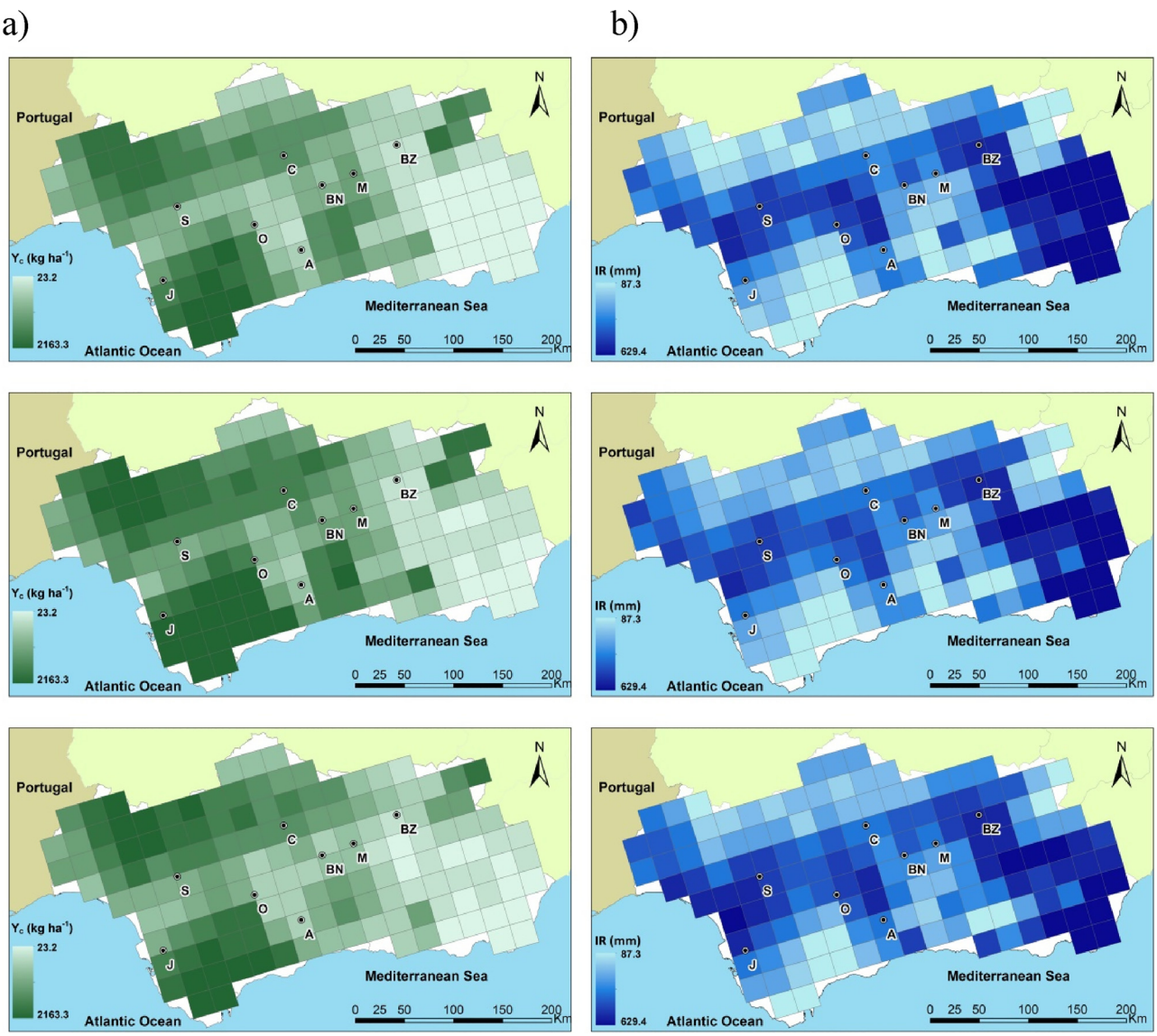

Fig. 8. Maps of simulated yield under rainfed conditions (Y_c; a) and irrigation water requirements (IR) under full irrigation strategy (R2; b) for baseline (top map), near future (middle) and far future (bottom) for DMI-BCM climate projection with 'Picual' cultivar and agronomic scenario described in Section 2.3. J, S, O, A, C, BN, M and BZ indicate the locations of Jerez, Sevilla, Osuna, Antequera, Córdoba, Baena, Martos and Baeza, respectively.

4. Discussion

The development of a specific simulation model for olive, named AdaptaOlive, based on experimental data from previous studies and considering key physiological components, enabled the evaluation of the response of olive yield, irrigation water requirements and economic projections to climate change under semi-arid conditions. The AdaptaOlive model constitutes an intermediate option between simple models (Rodríguez-Díaz et al., 2007; Quiroga and Iglesias, 2009; Tanasijevic et al., 2014) and full biophysically-based models (Morales et al., 2016) for assessing olive response under baseline and future climate conditions, avoiding the high level of detail required by some process-based models, which may mean their use is restricted to a local scale (Moriondo et al., 2015).

For the predicted future climate conditions in Andalusia, the mean olive yield will increase depending on irrigation availability; for the Baeza area, the change in yield was positive under both rainfed and irrigation conditions. The values of yield increase found are in agreement with or higher than those found in previous studies carried out by Viola et al. (2013, 2014) under rainfed conditions, and Morales et al. (2016) under irrigation, who reported an average increase in oil yield of around 7.7% under future climate conditions. Thus, the positive effects on olive transpiration efficiency of the crop stress (López-Bernal et al., 2015) and the increased atmospheric CO_2 (Tognetti et al., 2001) offset the negative impacts of climate change, such as the reduction in transpiration or the increase in water stress events during flowering (Gabaldón-Leal et al., 2017).

According to the AdaptaOlive model, future irrigation requirements are projected to decrease slightly under regulated deficit irrigation strategy. These results differ from the increases estimated by Rodríguez-Díaz et al. (2007), Tanasijevic et al. (2014) and Valverde et al. (2015), who projected average increases of around 20%. The differences detected were due to the inclusion in our model of the positive effects of the future reduction in crop transpiration, which reduced the irrigation requirements. The reduction of crop transpiration was due to the reduction in canopy conductance, caused by the increase in atmospheric CO_2 – a fact confirmed by numerous previous studies (Moriana et al., 2002; Villalobos and Fereres, 2004).

This study has shown the correlation between phenology and irrigation management, and damage caused by heat and water stress

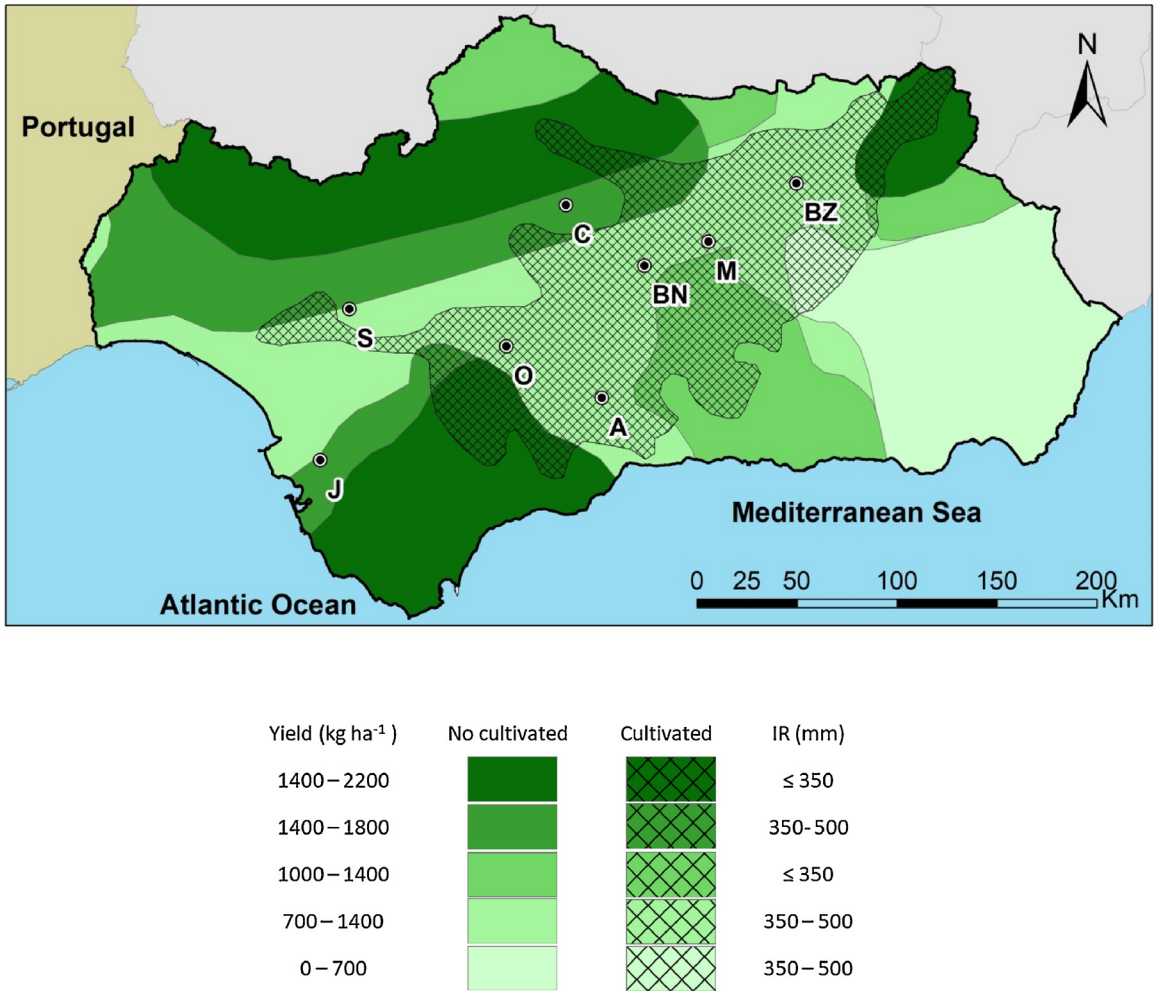

Fig. 9. Identification of areas in Andalusia with favorable and unfavorable production conditions considering yield values under rainfed conditions and full irrigation requirements for FF with DMI-BCM climate projection with 'Picual' cultivar and agronomic scenario described in Section 2.3. J, S, O, A, C, BN, M and BZ indicate the locations of Jerez, Sevilla, Osuna, Antequera, Córdoba, Baena, Martos and Baeza, respectively.

events, thus demonstrating the need for an accurate characterization of phenology under future weather conditions. Flowering is confirmed as a key phenological phase for the assessment of olive yield (Y_c), net margin (NM_c) and irrigation requirements (IR). Delays in flowering date under rainfed conditions resulted in additional damage caused by water stress. With deficit irrigation strategies, such delays led to increased irrigation requirements, a finding previously described by Senthilkumar et al. (2015), who reported reduced irrigation requirements with early flowering in maize. Despite its importance, phenology has been evaluated in relatively few studies examining the impact of climate change on olive development and growth (Galán et al., 2008; Gabaldón-Leal et al., 2017).

Our results indicate that climate change adaptation strategies for olive should be focused on promoting regulated deficit irrigation strategies, selecting early flowering cultivars, especially under rainfed conditions, and identifying new cultivation areas considering chilling hour needs, future water requirements and olive response under limited water availability. By applying these adaptation strategies, olive orchards under semi-arid conditions will not be dramatically affected in terms of yield, net income, water productivity or irrigation requirements. The promotion of deficit irrigation strategies, even with a very limited volumes (lower than 2000 $m^3 ha^{-1}$), is already considered an excellent adaptation strategy in a climate change scenario (Fereres and Soriano, 2007; Trentacoste et al., 2015). Other alternatives, such as rainfed or full irrigation for future periods, showed non-satisfactory results. Thus, under specific circumstances – such as when using reclaimed water, with irrigation water cost of over 1 € m^{-3} – full irrigation is unsustainable, with negative NM_c for many years. Under scenarios of high irrigation water cost and reduced olive oil price, common in many areas and years in Andalusia (e.g. in the Baeza area during the 2012 and 2014 seasons, irrigation water cost reached 0.48 € m^{-3} and oil yield price was 1.6 € kg^{-1}), economic analysis confirms that full irrigation is a non-optimal irrigation strategy, given that regulated deficit irrigation resulted in higher irrigation water productivity. In addition, deficit irrigation stabilized the net income year on year compared with rainfed conditions (where NM_c was negative for around 36% of the years), thus providing an additional advantage. Previous studies carried out by Fereres and Soriano (2007) or Iniesta et al. (2009) confirmed these results. Along with recommending regulated deficit irrigation strategies for olive, farmers should receive improved training by regional and local advisory services (Lorite et al., 2012; Iglesias and Garrote, 2015).

The selection of appropriate olive cultivars as a driving factor in phenological impacts, is also a key adaptation strategy, although only a few studies have addressed it (Koubouris et al., 2009; Orlandi et al., 2013). This study evaluated differences in irrigation requirements for regulated deficit irrigation (associated with changes in flowering dates) and in yield under rainfed conditions (associated with water stress during flowering). Thus, the assessment of irrigation requirements accounted for two predicted factors that were likely to have opposite effects on the crop: first, that ET_o will increase and rainfall will decrease; and second, that the flowering date (when irrigation is more

Table 5
Variation in rainfall (R), transpiration (T), irrigation requirements (IR), yield (Y_c), net margin (NM_c), water productivity (WP_c) and irrigation water productivity (IWP_c) for eight areas in Andalusia considering DMI_BCM climate projection with 'Picual' cultivar for far future period (FF) compared with baseline (B) period, for rainfed (R0C), deficit (R1) and full (R2) irrigation strategies.

Area	IS	R (%)	T (%)	IR (%)	Y_c (%)	NM_c (%)	WP_c (%)	IWP_c (%)
Antequera	R0C	−27.2	−31.7		−5.9	−8.1	64.8	
Seville	R0C	−22.1	−26.8		4.7	6.0	28.9	
Baena	R0C	−22.4	−27.3		−9.2	−11.9	14.2	
Martos	R0C	−22.7	−26.2		−9.3	−11.7	14.1	
Córdoba	R0C	−21.2	−27.9		−0.1	−0.1	26.9	
Baeza	R0C	−22.0	−22.2		−1.5	−2.1	32.8	
Osuna	R0C	−19.4	−22.8		2.6	3.3	27.8	
Jerez	R0C	−27.4	−32.7		−5.5	−6.9	20.5	
Antequera	R1	−27.2	−17.2	−0.7	26.1	37.1	57.8	69.7
Seville	R1	−22.1	−14.8	4.3	29.5	40.0	51.0	67.4
Baena	R1	−22.4	−16.3	2.4	25.0	34.2	47.1	82.0
Martos	R1	−22.7	−14.7	7.1	25.6	33.9	47.7	96.3
Córdoba	R1	−21.2	−16.1	4.6	27.1	36.2	50.1	91.7
Baeza	R1	−22.0	−12.7	−0.5	25.2	36.7	47.3	50.2
Osuna	R1	−19.4	−14.2	1.0	32.5	44.6	53.4	84.5
Jerez	R1	−27.4	−16.9	12.0	28.0	36.2	55.7	94.9
Antequera	R2	−27.2	−9.9	4.3	32.5	48.6	52.4	64.3
Seville	R2	−22.1	−10.2	0.8	33.7	51.5	50.3	66.5
Baena	R2	−22.4	−11.3	0.4	29.8	45.4	47.4	75.6
Martos	R2	−22.7	−10.9	1.4	29.2	43.7	47.6	86.8
Córdoba	R2	−21.2	−10.4	3.7	32.1	47.1	47.7	81.6
Baeza	R2	−22.0	−9.2	−1.2	28.8	46.1	46.0	50.2
Osuna	R2	−19.4	−10.1	−0.5	36.0	54.6	52.6	80.3
Jerez	R2	−27.4	−9.0	9.5	35.0	50.0	52.7	85.7

Table 6
Impact on simulated yield and net income of accounting for water stress in flowering (Y_w *vs.* Y_c and NM_w *vs.* NM_c) for rainfed conditions for baseline (B), near future (NF) and far future (FF) periods of the DMI_BCM climate projection and 'Picual' cultivar.

Location	Y_w *vs.* Y_c B (%)	Y_w *vs.* Y_c NF (%)	Y_w *vs.* Y_c FF (%)	NM_w *vs.* NM_c B (%)	NM_w *vs.* NM_c NF (%)	NM_w *vs.* NM_c FF (%)
Antequera	−14.1	−13.2	−21.5	−18.3	−16.5	−27.6
Seville	−7.3	−8.8	−12.5	−9.3	−10.9	−15.4
Baena	−6.5	−8.5	−21.9	−8.2	−10.5	−27.1
Martos	−3.5	−7.2	−20.5	−4.3	−8.8	−24.9
Córdoba	−3.1	−4.2	−11.6	−3.9	−5.1	−14.0
Baeza	−16.7	−20.8	−26.0	−22.7	−27.4	−34.2
Osuna	−6.4	−7.0	−19.8	−8.1	−8.4	−23.9
Jerez	−3.4	−5.6	−12.0	−4.2	−6.7	−14.7

critical) will occur earlier, and thus closer to the period of time with lower ET_o and more frequent rainfall. For the cultivars 'Arbequina', 'Picual', and 'Chiquitita' and the wild genotype 'FV18', the first of these two was the decisive factor, generating a steadily increasing trend of future irrigation requirements despite the earlier flowering dates. However, for late flowering 'GM22', the decisive factor was the flowering date, and its projected advance implied a reduction in irrigation requirements. When simulated yield under rainfed conditions was analyzed, 'GM22' showed the lowest values as the sensitive period (flowering) was delayed and so the probability of water stress damage increased compared with the rest of the genotypes. Similarly, although 'GM22' registered a high yield under the regulated deficit irrigation strategy, the higher probability of heat stress during flowering (Gabaldón-Leal et al., 2017) and the greater irrigation requirements make it an unsuitable choice. Finally, the genotypes under study behaved differently depending on the location, meaning that the impact of climate change may be exacerbated for some combinations of cultivars

Table 7
Simulated flowering date, irrigation requirements (IR), yield (Y_c), net margin (NM_c), water productivity (WP_c) and irrigation water productivity (IWP_c) for deficit irrigation strategy (R1) for five olive genotypes considered for baseline (B), near future (NF) and far future (FF) periods of the DMI-BCM climate projection, for the Baeza area.

Period	Genotype	Rainfall (mm)	Flowering date (DOY)	IR (mm)	Y_c (kg ha^{-1})	NM_c (€ ha^{-1})	WP_c (kg m^{-3})	IWP_c (kg m^{-3})
B	Arbequina	396.9	148	212.7	1876.3	2576.0	0.31	0.37
B	Picual	396.9	151	216.0	1885.1	2584.9	0.31	0.37
B	GM22	396.9	173	260.0	1994.3	2687.7	0.31	0.35
B	FV18	396.9	156	227.3	1918.1	2621.0	0.31	0.36
B	Chiquitita	396.9	152	218.0	1891.0	2591.5	0.31	0.37
NF	Arbequina	366.9	143	224.0	2179.6	3150.0	0.37	0.43
NF	Picual	366.9	146	225.3	2183.8	3155.0	0.37	0.43
NF	GM22	366.9	168	257.3	2283.4	3270.0	0.37	0.42
NF	FV18	366.9	152	234.7	2216.2	3195.2	0.37	0.43
NF	Chiquitita	366.9	148	230.7	2203.6	3180.6	0.37	0.43
FF	Arbequina	309.6	130	211.4	2345.1	3512.0	0.46	0.53
FF	Picual	309.6	133	215.0	2360.9	3534.2	0.46	0.53
FF	GM22	309.6	154	239.3	2464.6	3677.5	0.46	0.52
FF	FV18	309.6	138	221.4	2391.5	3578.4	0.46	0.53
FF	Chiquitita	309.6	134	218.6	2378.1	3559.3	0.46	0.53

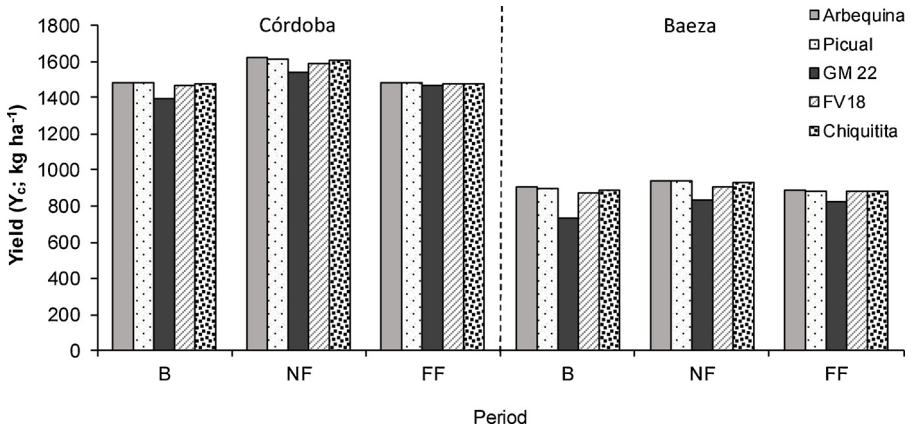

Fig. 10. Simulated yield considering the impact of water stress during flowering (Y_c) for five olive genotypes, two representative locations (Córdoba and Baeza), and three periods (B, NF and FF), considering DMI-BCM climate projection under rainfed conditions.

and locations (for example, with late flowering cultivars in dry locations), while cultivar selection is less important in temperate rainy locations.

Finally, the selection of appropriate new areas for olive cultivation is an additional potential adaptation strategy, which involves identifying areas with an adequate combination of rainfall and moderate temperatures. Some Andalusian areas such as the region of Jerez are very promising options for olive cultivation, as indicated by the highly satisfactory simulated yield, even under rainfed conditions, and with moderate irrigation requirements. However, an informed recommendation should take into account other aspects such as chilling hour requirements (Morales et al., 2016); Gabaldón-Leal et al. (2017) determined that the Jerez area would be affected by a lack of chilling hours in the future, leading to flowering failure, which in turn would severely impact olive yield. This illustrates how any adaptation strategy should be recommended with caution and only applied after a full site-specific examination of all the aspects involved. In this study, a detailed spatial analysis of the analyzed region revealed clear differences between areas, especially under rainfed conditions. This implies that spatially averaged values are not reliable impact indicators; instead, site-specific studies are required to demarcate those areas most severely impacted by climate change. However, under irrigation, Y_c and NM_c showed a more homogeneous spatial distribution as both the water stress during flowering and the effect of the uncertainty associated with precipitation projections were reduced (Sánchez and Miguez-Macho, 2010). This was because yield variability was primarily linked to variability in water availability, as previous studies have indicated (Giorgi et al., 2004). This fact was also observed when analyzing the inter-annual variability of oil yield under rainfed and irrigated conditions, with less variability as the irrigation supply increased.

One inherent concern in the use of climate projections for the identification of climate change impacts and adaptation measures is their variability according to the climate model considered (Mínguez et al., 2007), which represents an important source of uncertainty (Garrido et al., 2011). In our study, the consideration of an ensemble of 11 climate models allowed the assessment of uncertainty in the impact estimations carried out for future conditions, showing that the degree of uncertainty was especially high under rainfed conditions. In light of this fact, there is a clear need to consider an ensemble of climate models when assessing future climate impacts and adaptation strategies, in order to gauge both the average response and the divergences between estimates generated by different climate projections. In addition, the evaluation and bias correction (if needed) of the climate model outputs is advisable (Dosio et al., 2012; Ruiz-Ramos et al., 2015).

Regarding the reliability of the crop model, although this study includes several processes involved in the response of olive to climate change – such as increased atmospheric CO_2 and the impact of water stress on yield – some sources of uncertainty have not been fully addressed and thus require further study (Connor and Fereres, 2005). In addition, despite numerous valuable studies on olive under current conditions (Fernandez et al., 1997; Moriana et al., 2003; Tognetti et al., 2006; Berni et al., 2009; Villalobos et al., 2013), there is little information available on olive response under projected future climate. Thus, processes such as the impact of heat stress during flowering, changes in the duration of the flowering period, soil temperature effect, the reduction in radiation use efficiency with the age of the orchards (Morales et al., 2016) or the consideration of physiological processes specific to olive cultivars adapted to extremely stressful environments (Orlandi et al., 2013) have not been included in the approach proposed here. Similarly, the impact of the failure to meet chilling hour requirements (Morales et al., 2016) was omitted from the study due to the small probability of occurrence under the future climate conditions of most of the region of Andalusia and the high degree of uncertainty associated with the chilling hour requirements for olive (Gabaldón-Leal et al., 2017). Other processes not yet fully understood relate to the impact of climate change on the harvest index (HI) and on C_i/C_a, the acclimatization process of olive to high atmospheric CO_2 (Tognetti et al., 2001), the functions for representing the reduction in stomatal conductance with CO_2, and the impact of water stress on flowering (Connor, 2005). Likewise, some responses considered in this study, such as the increase in TE with water stress, were regarded as uncertain by Connor and Fereres (2005) and Moriana et al. (2002), who detected TE reductions in severely stressed olives.

For other crops such as wheat, the uncertainties associated with crop modeling are addressed by means of crop model ensembles (Pirttioja et al., 2015). However, this is not currently a feasible solution for olive due to the very limited number of models available. Thus, these limitations and uncertainties show the need for more olive experimentation under future climatic conditions, evaluating physiological processes outside of current meteorological ranges and analyzing interactions between such processes to develop more mechanistic models, able to capture the responses to multiple and interrelated environmental factors (Buckley and Mott, 2013).

5. Conclusions

A simulation model named AdaptaOlive, based on experimental data from previous studies, has been developed for evaluating key processes such as the response of transpiration, transpiration efficiency and yield to atmospheric CO_2 and crop water stress. This mechanistic simulation has enabled an assessment of olive response to climate model predictions of changes in weather conditions and atmospheric CO_2 in the Andalusia region during the 21st century.

Despite the predicted reduction in rainfall and the increases in heat

and water stress associated with increases in temperature, olive yield and irrigation water requirements in Andalusia would not be severely impacted. Thus, the positive response of olive to the increase in atmospheric CO_2 offsets the negative impacts of climate change on olive. As such, increases in mean yield are estimated, even under rainfed conditions. However, dry areas in the east of the region could be severely impacted by water stress during flowering, causing marked reductions in potential yield. To mitigate this impact, adaptation measures such as regulated deficit irrigation strategies have been evaluated with the AdaptaOlive model; results are excellent, showing average increases in yield of 28.9% at the end of this century. Other adaptation strategies involve the selection of early flowering cultivars (such as 'Arbequina'), as this means a lower probability of occurrence of water stress events during critical periods such as flowering; this strategy is therefore especially recommended under rainfed conditions.

The high degree of uncertainty affecting both impacts and adaptation has been addressed with site-specific analysis and by using an ensemble of 11 climate models. This uncertainty could be reduced even further by promoting the development of simulation models driven by new field experimentation, and considering key processes such as the interaction between water stress and the increase in CO_2 on olive under future climate conditions. Although some such advances have been achieved in this study, an intensive research effort is still required, especially for olive crops under semi-arid conditions.

Acknowledgements

This study has been financially supported by the project RTA2014-00030-00-00 funded by INIA, FEDER 2014–2020 "*Programa Operativo de Crecimiento Inteligente*", project AVA201601.2 funded by the European Regional Development Fund (FEDER), FACCE MACSUR – Modelling European Agriculture with Climate Change for Food Security, a FACCE JPI knowledge hub, and by MULCLIVAR, from the Spanish *Ministerio de Economía y Competitividad* (MINECO) CGL2012-38923-C02-02. The contributions of Dr. Orgaz and Dr. Moriana are highly appreciated.

Appendix A. Supplementary data

Supplementary data associated with this article can be found, in the online version, at https://doi.org/10.1016/j.agwat.2018.04.008.

References

Allen, R.G., Pereira, L.S., Raes, D., Smith, M., 1998. Crop Evapotranspiration: Guidelines for Computing Crop Water Requirements. Irrigation and Drainage Paper 56. United Nations, FAO, Rome.
Areal, F.J., Riesgo, L., 2014. Farmers' view on the future of olive farming in Andalusia, Spain. Land Use Policy 36, 543–553.
Ayerza, R., Sibbett, G.S., 2001. Thermal adaptability of olive (Olea europaea L.) to the Arid Chaco of Argentina. Agr. Ecosyst. Environ. 84, 277–285.
Bacelar, E.A., Santos, D.L., Moutinho-Pereira, J.M., Lopes, J.I., Gonçalves, B.C., Ferreira, T.C., Correia, C.M., 2007. Physiological behavior, oxidative damage and anti-oxidative protection of olive trees grown under different irrigation regimes. Plant Soil 292, 1–12.
Beer, C., Ciais, P., Reichstein, M., Baldocchi, D., Law, B.E., Papale, B.E., Soussana, J.F., Ammann, C., Buchmann, N., Frank, D., Gianelle, D., Janssens, I.A., Knohl, A., Köstner, B., Moors, E., Roupsard, O., Verbeeck, H., Vesala, T., Williams, C.A., Wohlfahrt, G., 2009. Temporal and among-site variability of inherent water use efficiency at the ecosystem level. Global Biogeochem. Cy. 23, GB2018.
Berni, J.A.J., Zarco-Tejada, P.J., Sepulcre-Canto, G., Fereres, E., Villalobos, F., 2009. Mapping canopy conductance and CWSI in olive orchards using high resolution thermal remote sensing imagery. Remote Sens. Environ. 113 (11), 2380–2388.
Brodribb, T., 1996. Dynamics of changing intercellular CO2 concentration (ci) during drought and determination of minimum functional ci. Plant Physiol. 111, 179–185.
Buckley, T.N., Mott, K.A., 2013. Modelling stomatal conductance in response to environmental factors. Plant Cell Environ. 36, 1691–1699.
Clarke, D., Smith, M., El-Askari, K., 1998. CropWat for Windows: User Guide. FAO, Rome.
Connor, D.J., Fereres, E., 2005. The physiology of adaptation and yield expression in olive. Hortic. Rev. 31.
Connor, D.J., 2005. Adaptation of olive (Olea europaea L.) to water-limited environments. Aus. J. Agric. Res. 56 (11), 1181–1189.
De Melo-Abreu, J.P., Barranco, D., Cordeiro, M., Tous, J., Rogado, B.M., Villalobos, F.J., 2004. Modelling olive flowering date using chilling for dormancy release and thermal time. Agric. For. Meteorol. 125, 117–127.
Dosio, A., Paruolo, P., 2011. Bias correction of the ENSEMBLES high-resolution climate change projections for use by impact models: evaluation on the present climate. J. Geophys. Res. 116, D16106.
Dosio, A., Paruolo, P., Rojas, R., 2012. Bias correction of the ENSEMBLES high resolution climate change projections for use by impact models: analysis of the climate changes signal. J. Geophys. Res. 117, D17110.
Drake, B.G., Gonzalez-Meler, M.A., Long, S.P., 1997. More efficient plants: a consequence of rising atmospheric CO2? Annu. Rev. Plant Physiol. Plant Mol. Biol. 48, 609–639.
Etheridge, D.M., Steele, L.P., Langenfelds, R.L., Francey, R.J., Barnola, J.M., Morgan, V.I., 1996. Natural and anthropogenic changes in atmospheric CO2 over the last 1000 years from air in Antarctic ice and firn. J. Geophys. Res. 101, 4115–4128.
Fereres, E., Soriano, M.A., 2007. Deficit irrigation for reducing agricultural water use. J. Exp. Bot. 58, 147–159.
Fernández-Escobar, R., de la Rosa, R., León, L., Gómez, J.A., Testi, L., Orgaz, F., Gil-Ribes, J.A., Quesada-Moraga, E., Trapero, A., 2013. Evolution and sustainability of the olive production systems, Options Méditerranéennes. Série A. Séminaires Méditerranéens 106, 11–42.
Fernandez, J.E., Moreno, F., Giron, I.F., Blazquez, O.M., 1997. Stomatal control of water use in olive tree leaves. Plant Soil 190 (2), 179–192.
Field, C.B., Jackson, R.B., Mooney, H.A., 1995. Stomatal responses to increased CO2: implications from the plant to the global scale. Plant Cell Environ. 18, 1214–1225.
Gómez del Campo, M., 2013. Summer deficit-irrigation strategies in a hedgerow olive orchard cv. 'Arbequina': effect on fruit characteristics and yield. Irrig. Sci. 31, 259–269.
Gómez-Limón, J.A., Riesgo, L., 2010. Sustainability assessment of olive grove in Andalusia: a methodological proposal. In: 120th EAAE Seminar External Cost of Farming Activities: Economic Evaluation, Environmental Repercussions and Regulatory Framework. Crete, Greece.
Gabaldón-Leal, C., Ruiz-Ramos, M., de la Rosa, R., León, L., Belaj, A., Rodriguez, A., Santos, C., Lorite, I.J., 2017. Impact of changes in mean and extreme temperatures caused by climate change on olive flowering in southern Spain. Int. J. Climatol. 37 (S1), 940–957.
Galán, C., García-Mozo, H., Vázquez, L., Ruiz-Valenzuela, L., Díaz de la Guardia, C., Dominguez-Vilches, E., 2008. Modeling olive crop yield in Andalusia, Spain. Agron. J. 100 (1), 98–104.
Garrido, A., Rey, D., Ruiz-Ramos, M., Mínguez, M.I., 2011. Climate change and crop adaptation in Spain: consistency of regional climate models. Clim. Res. 49, 211–227.
Giorgi, F., Bi, X., Pal, J., 2004. Mean, interannual variability and trends in a regional climate change experiment over Europe. II: climate change scenarios (2071–2100). Clim. Dynam. 23, 839–858.
Herrera, S., Gutiérrez, J.M., Ancell, R., Pons, M.R., Frías, M.D., Fernández, J., 2012. Development and analysis of a 50-year high-resolution daily gridded precipitation dataset over Spain (Spain02). Int. J. Climatol. 32, 74–85.
Iglesias, A., Garrote, L., 2015. Adaptation strategies for agricultural water management under climate change in Europe. Agric. Water Manage. 155, 113–124.
Iniesta, F., Testi, L., Orgaz, F., Villalobos, F.J., 2009. The effects of regulated and continuous deficit irrigation on the water use, growth and yield of olive trees. Eur. J. Agron. 30 (4), 258–265.
Koubouris, G.C., Metzidakis, I.T., Vasilakakis, M.D., 2009. Impact of temperature on olive (Olea europaea L.) pollen performance in relation to relative humidity and genotype. Environ. Exp. Bot. 67, 209–214.
López-Bernal, A., García-Tejera, O., Vega, V.A., Hidalgo, J.C., Testi, L., Orgaz, F., Villalobos, F.J., 2015. Using sap flow measurements to estimate net assimilation in olive trees under different irrigation regimes. Irrig. Sci. 33, 357–366.
Lanzas, J.R., Moral, E., 2008. Situación actual del sector del aceite de oliva. In: de Andalucía, Analistas Económicos (Ed.), Informe Anual del Sector Agrario en Andalucía 2008. Analistas Económicos de Andalucía, Málaga, pp. 543–575.
Lorite, I.J., García-Vila, M., Carmona, M.A., Santos, C., Soriano, M.A., 2012. Assessment of the Irrigation Advisory Services' recommendations and farmers' irrigation management: a case study in Southern Spain. Water Resour. Manage. 26, 2397–2419.
Mínguez, M.I., Ruiz-Ramos, M., Díaz-Ambrona, C.H., Quemada, M., Sau, F., 2007. First-order impacts on winter and summer crops assessed with various high-resolution climate models in the Iberian Peninsula. Clim. Change 81, 343–355.
Meek, D.W., Hatfield, J.L., Howell, T.A., Idso, S.B., Reginato, R.J., 1984. A generalized relationship between photosynthetically active radiation and solar radiation. Agron. J. 76, 939–945.
Mesa-Jurado, M.A., Berbel, J., Orgaz, F., 2010. Estimating marginal value of water for irrigated olive grove with the production function method. Span. J. Agric. Res. 8 (82), S197–S206.
Monteith, J.L., 1965. Light distribution and photosynthesis in field crops. Ann. Bot. 29, 17–37.
Morales, A., Leffelaar, P.A., Testi, L., Orgaz, F., Villalobos, F.J., 2016. A dynamic model for potential growth of olive (Olea europaea L.) orchards. Eur. J. Agron. 74, 93–102.
Moriana, A., Villalobos, F.J., Fereres, E., 2002. Stomatal and photosynthetic responses of olive (Olea europaea L.) leaves to water deficits. Plant Cell Environ. 25, 395–405.
Moriana, A., Orgaz, F., Pastor, M., Fereres, E., 2003. Yield responses of a mature olive orchard to water deficits. J. Am. Soc. Hort. Sci. 128 (3), 425–431.
Moriondo, M., Ferrise, R., Trombi, G., Brilli, L., Dibari, C., Bindi, M., 2015. Modelling olive trees and grapevines in a changing climate. Environ. Modell. Softw. 72, 387–401.
Nakićenović, N., Alcamo, J., Davis, G., de Vries, B., Fenhann, J., Gaffin, S., Gregory, K., Grubler, A., Jung, T.Y., Kram, T., La Rovere, E.L., Michaelis, L., Mori, S., Morita, T., Pepper, W., Pitcher, H., Price, L., Riahi, K., Roehrl, A., Rogner, H.H., Sankoyski, A.,

Schlesinger, M., Shukla, P., Smith, S., Swart, R., van Rooijen, S., Victor, N., Zhou, D., 2000. In: Nakićenović, N., Swart, R. (Eds.), Special Report on Emissions Scenarios (SRES). Cambridge Univ. Press, Cambridge.
Orgaz, F., Fereres, E., 2004. Riego. In: Barranco, D., Fernández-Escobar, R., Rallo, L. (Eds.), El cultivo del olivo, 4th edition. Junta de Andalucía – Ediciones Mundiprensa, pp. 285–306.
Orgaz, F., Testi, L., Villalobos, F.J., Fereres, E., 2006. Water requirements of olive orchards: II: determination of crop coefficients for irrigation scheduling. Irrig. Sci. 24, 77–84.
Orlandi, F., Avolio, E., Bonofiglio, T., Federico, S., Romano, B., Fornaciari, M., 2013. Potential shifts in olive flowering according to climate variations in Southern Italy. Meteorol. Appl. 20, 497–503.
Osborne, C.P., Chuine, I., Viner, D., Woodward, F.I., 2000. Olive phenology as a sensitive indicator of future climatic warming in the Mediterranean. Plant Cell Environ. 23, 701–710.
Oteros, J., García-Mozo, H., Vázquez, L., Mestre, A., Domínguez-Vilches, E., Galán, C., 2013. Modelling olive phenological response to weather and topography. Agric. Ecosyst. Environ. 179, 62–68.
Parras, M., 2013. New global and local marketing strategies: creation of added value though differentiation and high quality products. Options Mediterraneennes: Serie A. Seminaires Mediterraneens 106, 87–95.
Pirttioja, N., Carter, T.R., Fronzek, S., Bindi, M., Hoffmann, H., Palosuo, T., Ruiz-Ramos, M., Tao, F., Trnka, M., Acutis, M., Asseng, S., Baranowski, P., Basso, B., Bodin, P., Buis, S., Cammarano, D., Deligios, P., Destain, M.F., Dumont, B., Ewert, F., Ferrise, R., François, L., Gaiser, T., Hlavinka, P., Jacquemin, I., Kersebaum, K.C., Kollas, C., Krzyszczak, J., Lorite, I.J., Minet, J., Minguez, M.I., Montesino, M., Moriondo, M., Müller, C., Nendel, C., Öztürk, I., Perego, A., Rodríguez, A., Ruane, A.C., Ruget, F., Sanna, M., Semenov, M.A., Slawinski, C., Stratonovitch, P., Supit, I., Waha, K., Wang, E., Wu, L., Zhao, Z., Rötter, R.P., 2015. Temperature and precipitation effects on wheat yield across a European transect: a crop model ensemble analysis using impact response surfaces. Clim. Res. 65, 87–105.
Quiroga, S., Iglesias, A., 2009. A comparison of the climate risk of cereal, citrus, grapevine and olive production in Spain. Agric. Syst. 101, 91–100.
Raes, D., Steduto, P., Hsiao, T.C., Fereres, E., 2013. Reference Manual AquaCrop Version 4.0. FAO, Rome.
Rallo, L., Barranco, D., de la Rosa, R., León, L., 2008. 'Chiquitita' olive. HortScience 43, 529–531.
Rapoport, H.F., Hammami, S.B.M., Martins, P., Pérez-Priego, O., Orgaz, F., 2012. Influence of water deficits at different times during olive tree inflorescence and flower development. Environ. Exp. Bot. 77, 227–233.
Rodríguez-Díaz, J.A., Weatherhead, E.K., Knox, J.W., Camacho, E., 2007. Climate change impacts on irrigation water requirements in the Guadalquivir river basin in Spain. Reg. Environ. Chang. 7, 149–159.
Ruiz-Ramos, M., Sánchez, E., Gallardo, C., Mínguez, M.I., 2011. Impacts of projected maximum temperature extremes for C21 by an ensemble of regional climate models on cereal cropping systems in the Iberian Peninsula. Nat. Hazards Earth Syst. Sci. 11, 3275–3291.
Ruiz-Ramos, M., Rodríguez, A., Dosio, A., Goodess, C.M., Harpham, C., Mínguez, M.I., Sánchez, E., 2015. Comparing correction methods of RCM outputs for improving crop impact projections in the Iberian Peninsula for 21st century. Clim. Change 134, 283–297.
Ruiz-Ramos, M., Ferrise, R., Rodríguez, A., Lorite, I.J., Bindi, M., Carter, T.R., Fronzek, S., Talosuo, T., Pirttioja, N., Baranowki, P., Buis, S., Cammarano, D., Chen, Y., Dumont, B., Ewert, F., Gaiser, T., Hlavinka, P., Hoffmann, H., Höhn, J.G., Jurecka, F., Kersebaum, K.C., Krzyszczak, J., Lana, M., Mechiche-Alami, A., Minet, J., Montesino, M., Nendel, C., Porter, J.R., Ruget, F., Semenov, M.A., Steinmetz, Z., Stratonovitch, P., Supit, I., Tao, F., Trnka, M., de Wit, A., Rötter, R.P., 2018. Adaptation response surfaces for managing wheat under perturbed climate and CO2 in a Mediterranean environment. Agric. Syst. 159, 260–274.
Sánchez, E., Miguez-Macho, G., 2010. Proyecciones regionales de clima sobre la Península Ibérica: modelización de escenarios de cambio climático. Pérez, F. Fiz, Roberta, Boscolo (Eds.), Clima en España: pasado, presente y futuro 69–80.
Sanchez-Martinez, J.D., Paniza, A., 2015. The olive monoculture in the south of Spain. Eur. J. Geogr. 6 (3), 16–29.
Santos, C., Lorite, I.J., Allen, R.G., Tasumi, M., 2012. Aerodynamic parameterization of the satellite-based energy balance (METRIC) model for ET estimation in rainfed olive orchards of Andalusia, Spain. Water Resour. Manage. 26, 3267–3283.
Senthilkumar, K., Bergez, J.E., Leenhardt, D., 2015. Can farmers use maize earliness choice and sowing dates to cope with future scarcity? A modelling approach applied to south-western France. Agric. Water Manage. 152, 125–134.
Tanasijevic, L., Todorovic, M., Pereira, L.S., Pizzigalli, C., Lionello, P., 2014. Impacts of climate change on olive crop evapotranspiration and irrigation requirements in the Mediterranean region. Agric. Water Manage. 144, 54–68.
Tognetti, R., Sebastiani, L., Vitagliano, C., Raschi, A., Minnocci, A., 2001. Responses to two olive tree (Olea europaea L.) cultivars to elevated CO2 concentration in the field. Photosynthetica 39 (3), 403–410.
Tognetti, R., Sebastiani, L., Minnocci, A., Raschi, A., 2002. Foliar responses of olive trees (Olea Europaea L.) under field exposure to elevated CO2 concentration. In: Vitagliano, C., Martelli, G.P. (Eds.), Proc. 4th IS on Olive Growing. Acta Hort. 586, ISHS.
Tognetti, R., d'Andria, R., Lavini, A., Morelli, G., 2006. The effect of deficit irrigation on crop yield and vegetative development of Olea europaea L. (cvs. Frantoio and Leccino). Eur. J. Agron. 25 (4), 356–364.
Trentacoste, E.R., Puertas, C.M., Sadras, V.O., 2015. Effect of irrigation and tree density on vegetative growth oil yield and water use efficiency in young olive orchard under arid conditions in Mendoza, Argentina. Irrig. Sci. 33, 429–440.
Valverde, P., Serralheiro, R., de Carvalho, M., Maia, R., Oliveira, B., Ramos, V., 2015. Climate change impacts on irrigated agriculture in the Guadiana river basin (Portugal). Agric. Water Manage. 152, 17–30.
Villalobos, F.J., Fereres, E., 2004. Climate change effects on crop water requirements in southern Spain. I. Evapotranspiration. In: Jacobsen, S.E., Jensen, C.R., Porter, J.R. (Eds.), Proceedings of VIII Congress of the European Society of Agronomy. KVL, Copenhagen. pp. 347–348.
Villalobos, F.J., Testi, L., Hidalgo, J., Pastor, M., Orgaz, F., 2006. Modelling potential growth and yield of olive (Olea europaea L.) canopies. Eur. J. Agron. 24, 296–303.
Villalobos, F.J., Perez-Priego, O., Testi, L., Morales, A., Orgaz, F., 2012. Effects of water supply on carbon and water exchange of olive trees. Eur. J. Agron. 40, 1–7.
Villalobos, F.J., Testi, L., Orgaz, F., García-Tejera, O., López-Bernal, A., González-Dugo, M.A., Ballester-Lurbe, C., Castel, J.R., 2013. Modelling canopy conductance and transpiration of fruit trees in Mediterranean areas: a simplified approach. Agric. For. Meteorol. 171–172, 93–103.
Viola, F., Caracciolo, D., Pumo, D., Noto, L.V., 2013. Olive yield and future climate forcings. Procedia Environ. Sci. 19, 132–138.
Viola, F., Caracciolo, D., Pumo, D., Noto, L.V., La Loggia, G., 2014. Future climate forcings and olive yield in a Mediterranean orchard. Water 6, 1562–1580.